Supporting Information

Green-Solvent-Processable Polymer Hole Transport Material for Achieving 26.31% Efficiency in Inverted Perovskite Solar Cells

*Sen Yin, Xuanang Luo, Fushen Tang, Zhihui Xiong, Youran Lin, Wenyu Yang, Yuanyuan Shu, Yang Wang and Lei Ying**

Institute of Polymer Optoelectronic Materials and Devices Guangdong Basic Research Center of Excellence for Energy and Information Polymer Materials State Key Laboratory of Luminescent Materials and Devices South China University of Technology Guangzhou 510640, China.

E-mail: msleiying@scut.edu.cn

Experimental Section

1. Materials Synthesis

All the starting chemicals for materials synthesis were purchased from Dongguan Volt-Amp Optoelectronics Tech Co. Ltd. (China) and used without further purification. Compound M1 and M2 was synthesized by following the previous literature.[1] Lead iodide (PbI_2) and lead bromide ($PbBr_2$) were purchased from TCI. Formamidinium iodide (FAI), cesium iodide (CsI), methylammonium bromide (MABr), methylamine hydrochloride (MACl) and piperazinium iodide (PI) were purchased from Xi'an Yuri Solar Co., Ltd. (China). The synthetic route of monomers and polymer HTMs were shown in Fig. S1.

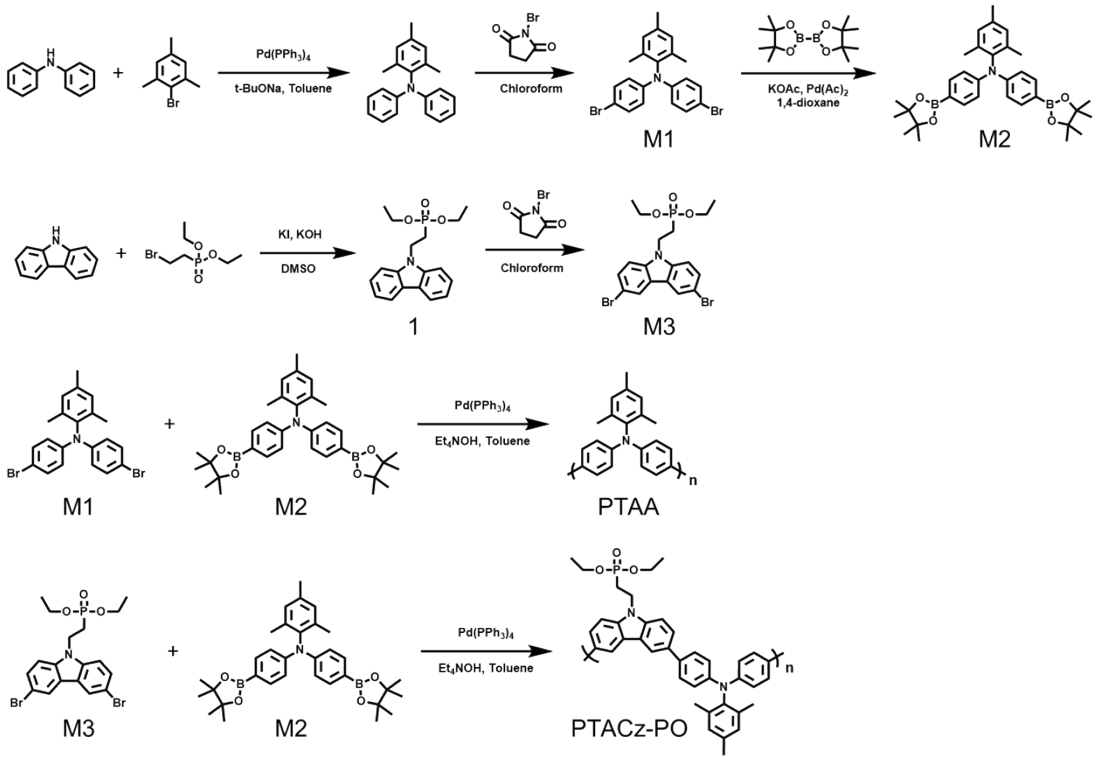

Figure S1. Synthesis route of the monomers and polymers.

Polymerization of poly[bis(4-phenyl)(2,4,6-trimethylphenyl)amine] (PTAA)

M1 (250.0 mg, 0.56 mmol) and M2 (302.8 mg, 0.56 mmol) were dissolved in 4 mL toluene in a N_2 atmosphere. $Pd(PPh_3)_4$ (33.1 mg) and Et_4NOH (250.0 mg) were then added. The reaction was conducted at 120 °C for 24 hours under nitrogen protection.

The resulting product was collected by precipitation into methanol. The crude polymer was purified using Soxhlet extraction with methanol, acetone, hexane, and chlorobenzene in order. The chlorobenzene fraction was further purified by silica chromatography using chlorobenzene as the eluent, resulting in a pale-yellow solid with a 66% yield.

Synthesis of diethyl [2-(9H-carbazol-9-yl)ethyl]phosphonate (1)

9H-carbazole (2.00 g, 11.96 mmol), diethyl (2-bromoethyl)phosphonate (5.86 g, 23.92 mmol), potassium iodide (0.40 g) and potassium hydroxide (5.00 g) were dissolved in 150 mL dimethyl sulfoxide (DMSO) inside a 500 mL flask. The reaction was conducted under nitrogen at 50 °C for 24 hours. Subsequently, the product was washed with deionized water and precipitated into methanol. The product was further purified by recrystallization using a mixture of methanol and dichloromethane, yielding a 84% final product. ^{1}H NMR (500 MHz, DMSO-*d*) δ 8.16 (d, 2H), 7.58 (d, 2H), 7.49 – 7.45 (t, 2H), 7.23 – 7.20 (t, 2H), 4.63 – 4.56 (m, 2H), 3.94 – 3.87 (m, 4H), 2.32 – 2.24 (m, 2H), 1.22 – 1.08 (t, 6H). ^{13}C NMR (101 MHz, DMSO -*d*) δ 139.93, 126.18, 122.77, 120.73, 119.43, 109.68, 61.64, 61.58, 37.06, 37.03, 25.40, 24.05, 16.53, 16.47.

Synthesis of diethyl (2-(3,6-dibromo-9H-carbazol-9-yl)ethyl)phosphonate (M3)

Compound 1 (1.00 g, 3.02 mmol) was dissolved in 40 mL chloroform inside a 150 mL flask. 1-bromopyrrolidine-2,5-dione (1.13 g, 6.34 mmol) was separately dissolved in 20 mL of chloroform and added dropwise to the flask under dark conditions. The reaction was carried out under nitrogen at 30 °C for 6 hours. Then, the product was washed with a sodium bicarbonate solution and collected by precipitation into methanol. The product was further purified by silica chromatography using ethyl acetate and petroleum ether as the eluent with a yield of 78%.^{1}H NMR (400 MHz, Chloroform-*d*) δ 8.13 (d, 2H), 7.58 (dd, 2H), 7.32 (d, 2H), 4.59 – 4.54 (m, 2H), 4.07 – 4.01 (m, 4H), 2.26 – 2.20 (m, 2H), 1.26 – 1.23 (t, 6H). ^{13}C NMR (126 MHz, Chloroform-*d*) 138.68, 129.28, 123.74, 123.40, 112.52, 110.31, 62.02, 61.97, 37.27,

25.76, 24.66, 16.37, 16.32.

Polymerization of PTACz-PO

The polymerization of PTACz-PO was carried out following the same procedure as for PTAA, yielding pale solids with yields of 44%.

Attempts to hydrolyze the PO groups in PTACz-PO resulted in an insoluble product. Furthermore, the incomplete conversion of the phosphate to phosphonic acid during hydrolysis complicates the determination of the polymer's exact state and may affect batch stability, as reported in recent studies on related polymers[2, 11, 18, 19].

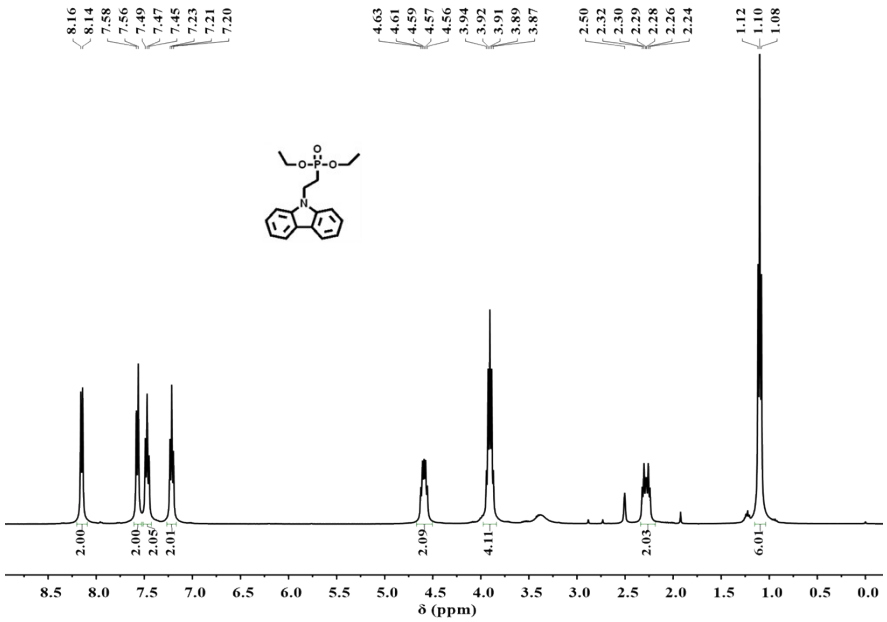

Figure S2. ^{1}H NMR spectrum of compound 1.

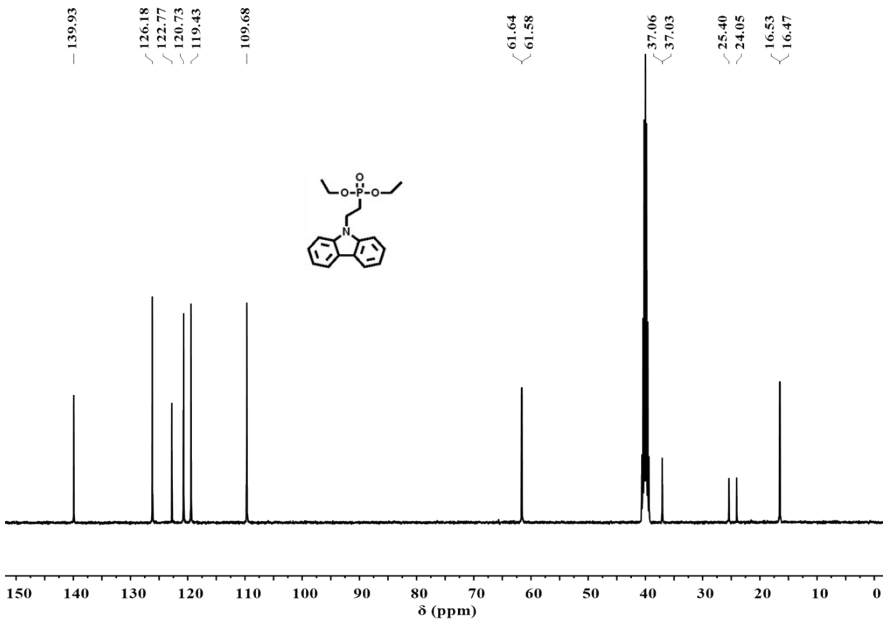

Figure S3. ^{13}C NMR spectrum of compound 1.

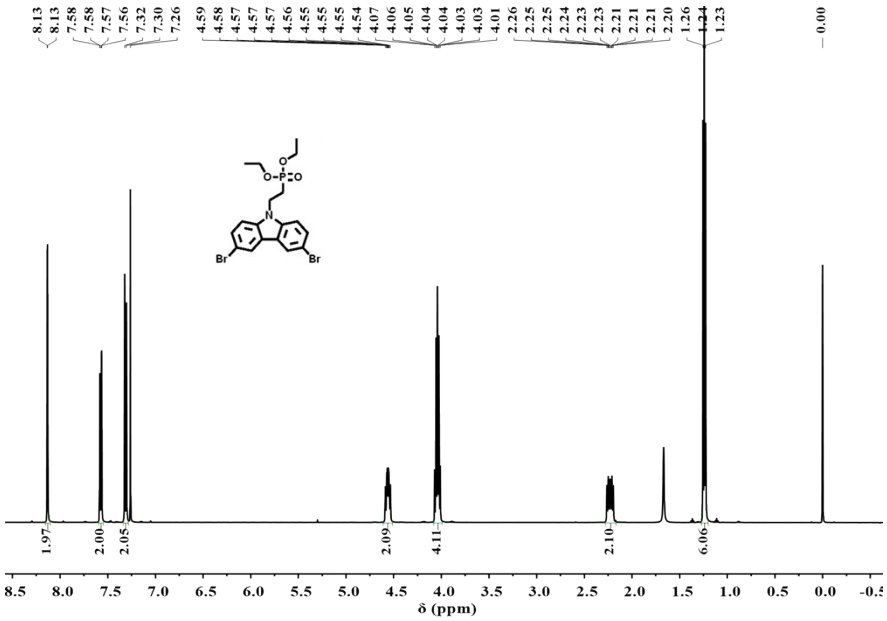

Figure S4. ^{1}H NMR spectrum of compound 2.

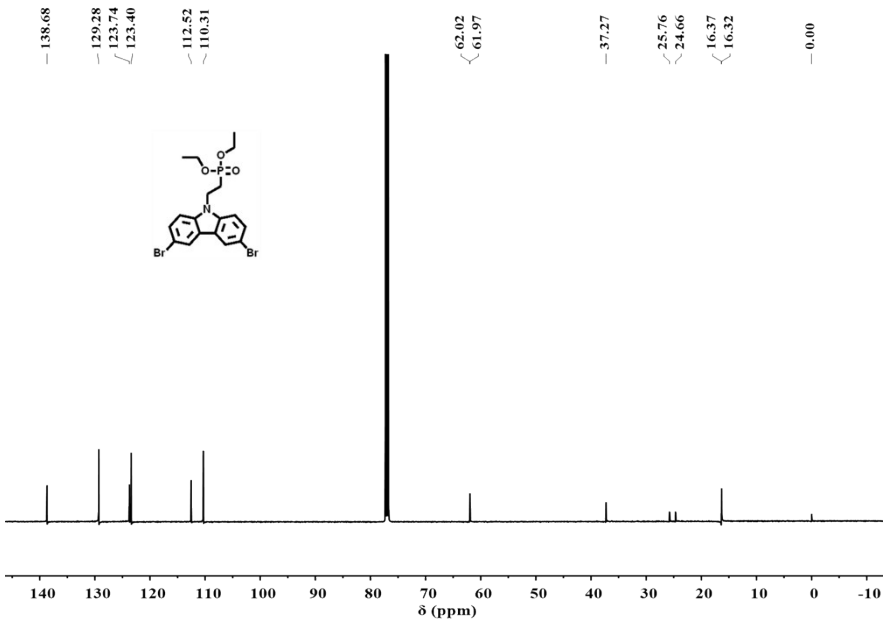

Figure S5. ^{13}C NMR spectrum of compound 2.

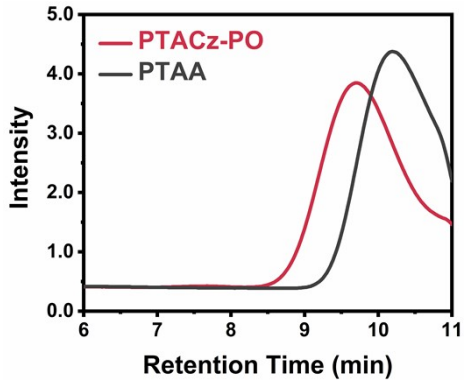

Figure S6. GPC elution curves of the PTAA and PTACz-PO.

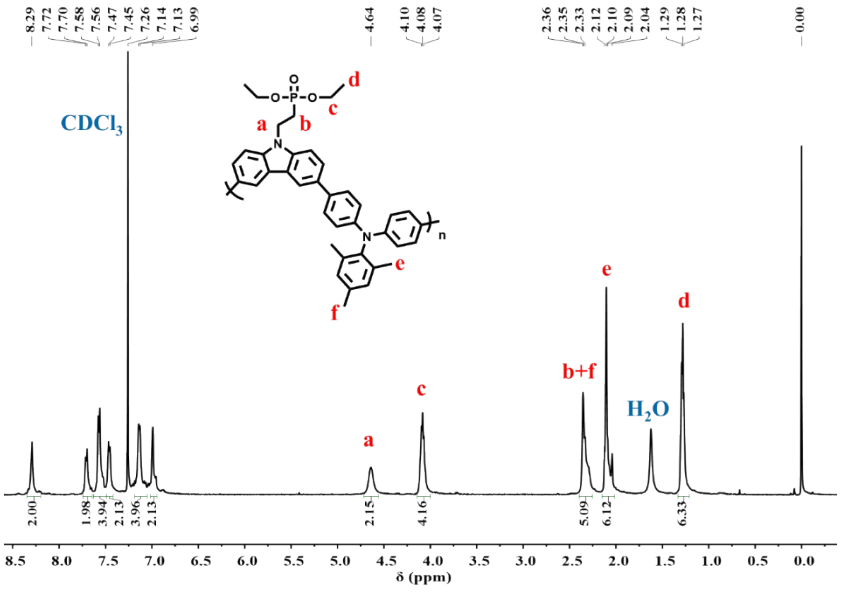

Figure S7. ^{1}H NMR spectrum of PTACz-PO scraped from the ITO/PTACz-PO substrate.

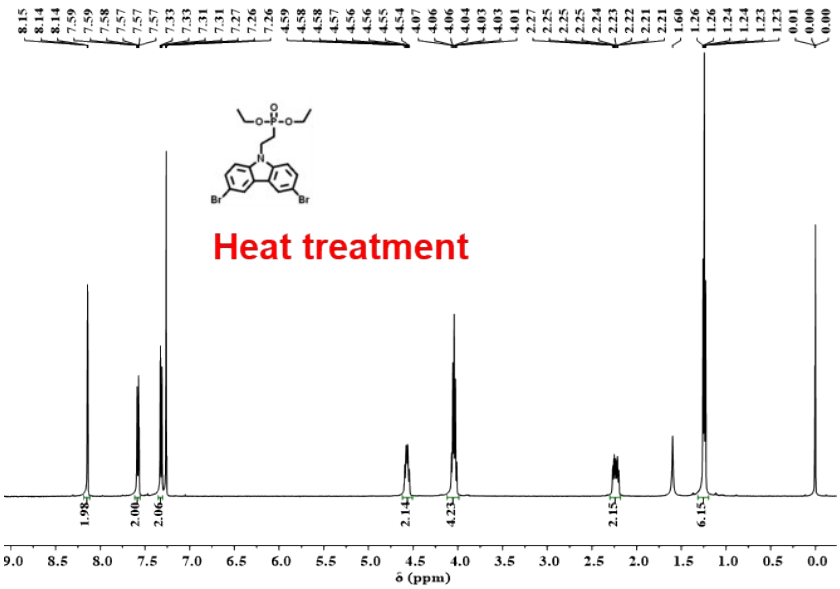

Figure S8. ^{1}H NMR spectrum of the monomer Cz-PO after heat treatment.

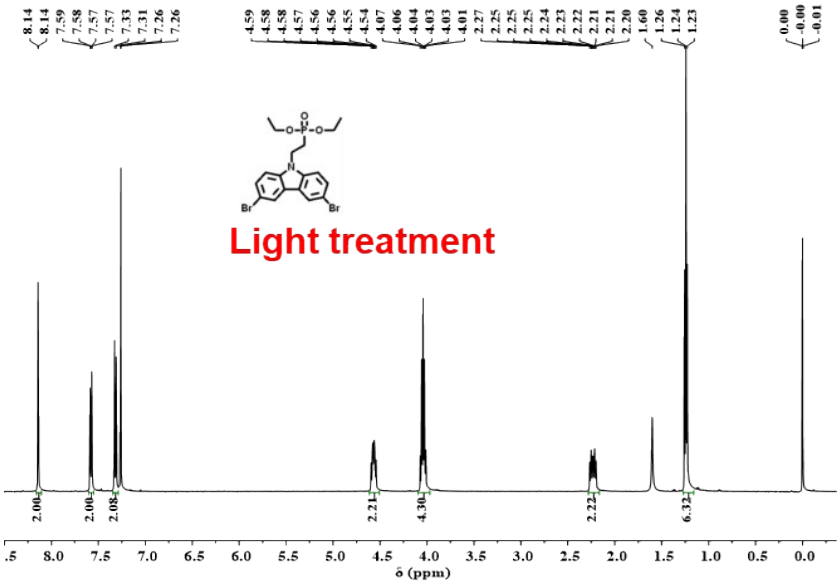

Figure S9. ^{1}H NMR spectrum of the monomer Cz-PO after light treatment.

2. General characterizations

NMR measurements were performed using a Bruker AVANCE 400/500 spectrometer operating at 400 or 500 MHz, with tetramethylsilane (TMS) as the internal

standard. UV-vis absorption spectra of the thin films, spin-cast on quartz glass, were recorded using a Shimadzu UV-3600 UV-vis-NIR spectrometer. PL and PL decay spectra were collected by FLS980 (Edinburgh Instrument, UK). UPS and XPS measurements were conducted on an Axis Supra+ (Kratos), with Ag as the reference. The contact angle tests for thin films were performed on an OCA50 contact angle goniometer, using dimethyl sulfoxide and diiodomethane. Surface energy was calculated with the Owens-Wendt-Rabel-Kaelble (OWRK) method. Field emission scanning electron microscope (FESEM) top surface, bottom surface and cross-section images of the perovskites were obtained on a SU8600 FESEM, Hitachi. Tapping-mode AFM images were obtained on a Bruker Multimode 8 Microscope. Kelvin probe force microscopy (KPFM) were acquired by Cypher ES (Oxford Instruments Asylum Research) via AC mode at 2.44 Hz with ASYELEC.01-R2 probe. X-ray diffraction (XRD) characterization was carried out in a x'pert3 powder, PANalytical B.V.

3. Simulations

The dimer molecular structures for various polymers were optimized by density functional theory (DFT) through Gaussian package, using the B3LYP-D3/6-31G** method. Electrostatic potential (ESP) and dipole moments were calculated and illustrated using Gaussian with B3LYP-D3/def-TZVP.

For the calculations of reorganization energy of molecular models for polymers, the excited-state structure was optimized using UB3LYP-D3/6-31G**, and the structural relaxation was visualized using VMD software. The four single-point energies of the ground-state structure (with 0 and 1 charge) and the excited-state structure (with 0 and 1 charge) were calculated using (U)B3LYP-D3/6-311G**. The energy differences for the structures with 0 and 1 charges are referred to as $\lambda 1$ and $\lambda 2$, respectively, and their sum represents the reorganization energy.

The electron density difference (EDD) was obtained from DFT-optimized polymer units with forcite and calculated using GGA/PBE via CASTEP.

Hansen solubility parameters of polymer HTMs were defined by δ_D, δ_P, δ_H and R_0,

obtained by using HSPIP software to fit the solubility of the solute in different solvents with known solubility parameters. Furthermore, Ra is defined as the radius of interaction, which is calculated from using eq (1).

$$Ra^2 = 4(\delta_{D1} - \delta_{D2})^2 + (\delta_{P1} - \delta_{P2})^2 + (\delta_{H1} - \delta_{H2})^2 \quad (1)$$

1 and 2 in the subscripts represent the solute and solvent, respectively.

4. Device fabrication and characterizations

For the preparation of $Cs_{0.05}(FA_{0.95}MA_{0.05})_{0.95}Pb(I_{0.95}Br_{0.05})_3$, a 1.5 M perovskite precursor solution was prepared by mixing CsI, FAI, PbI_2, MABr and $PbBr_2$ in a DMF: DMSO = 4:1(vol/vol) solvent mixture according to the stoichiometric ratio. The solution was stirred for 12 hours, with an additional 3 mol% PbI_2 and 10 mol% MACl added to improve crystallization.

The inverted perovskite solar cell fabrication involved the following steps: Glass/ITO substrates were cleaned by sonication with detergent, deionized water and isopropyl alcohol for 20 min, followed by drying at 70 °C. Before use in the glove box, the substrates were treated with oxygen plasma for 10 min. The polymer HTM solution (3 mg/ml PTAA in chlorobenzene, 3 mg/ml PTACz-PO in chlorobenzene and 3 mg/ml PTACz-PO in 2-methyltetrahydrofuran) was spin-coated onto the ITO substrates at 4000 rpm for 30 s, followed by annealing at 100 °C for 10 min. The thicknesses of PTAA, CB-processed PTACz-PO, and MeTHF-processed PTACz-PO films were 26 nm, 22 nm and 21 nm, respectively, demonstrating the robustness of the HTLs during processing. For the perovskites layer, perovskite precursor solution was spin-coated onto glass/ITO/HTM substrate at 5000 rpm for 40 s, 200 μL chlorobenzene was dripped onto the center of film at 12 s before the end of spin coating, followed by annealing on a hotplate at 110 ℃ for 30 min. A piperazine hydroiodide solution (0.3 mg mL^{-1} in isopropyl alcohol) was spin-coated onto the perovskite film at 5000 rpm for 30 s and annealed at 100 °C for 5 minutes. Then, a 20 nm C60, 7 nm BCP and 100 nm silver were thermally evaporated under high vacuum (<4 × 10^{-6} Torr) sequentially.

The current density-voltage (*J-V*) curves of the devices were measured using a Keithley 2400 sourcemeter under 1 sun irradiation from an AM 1.5 G solar simulator

(SS-F5, Enlitech). External quantum efficiency (EQE) spectra were obtained using an EQE measurement system (QE-R, Enlitech), calibrated with a standard single-crystal Si photodetector before testing. The electrochemical impedance spectroscopy (EIS) spectra were tested at room temperature, using an impedance analyzer (Keysight E4990A).

Hole-only devices to evaluate the charge transport for polymers were fabricated with ITO/PEDOT:PSS/polymer/MoO_3/Ag. The *J-V* curves of the devices were recorded using a Keithley 236 sourcemeter. The mobility was determined by SCLC method according to the Mott-Gurney equation, expressed as $J = 9\varepsilon_0\varepsilon_r\mu V^2/8d^3$, where J is the current density, ε_0 is the vacuum permittivity, ε_r is the relative permittivity, μ is the charge mobility, and d is the thickness of the polymer.

Hole-only devices to evaluate the trap density for perovskites deposited on various polymer hole transport layer were fabricated with ITO/polymer/perovskite/Spiro-OMeTAD/Ag. The defect density N_t can be obtained by equation: $N_t = 2\varepsilon_0\varepsilon V_{TFL}/qL^2$, where ε and ε_0 are the relative dielectric constant and vacuum permittivity. V_{TFL} is the onset voltage of TFL region, and q and L are elementary charge and the thickness of perovskite layer, respectively.

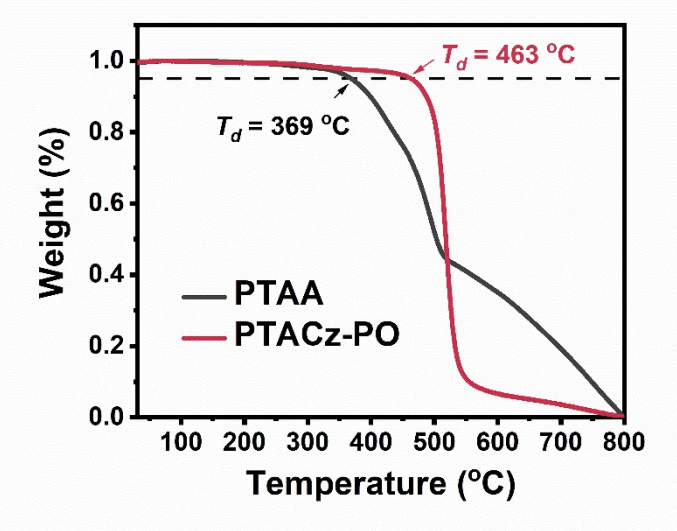

Figure S10. TGA plots of polymer PTACz-PO and PTAA with a heating rate of 10 °C min^{-1} under an insert atmosphere.

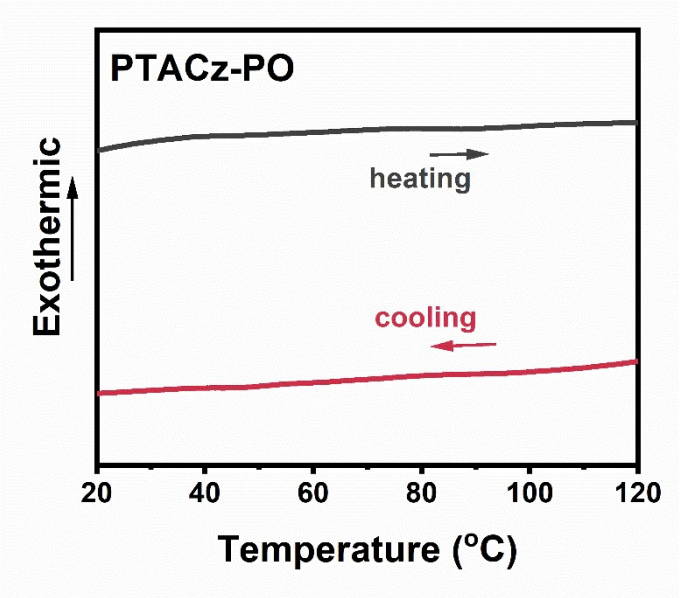

Figure S11. DSC diagrams of polymer PTACz-PO at a ramp rate of 10 ℃ min^{-1}.

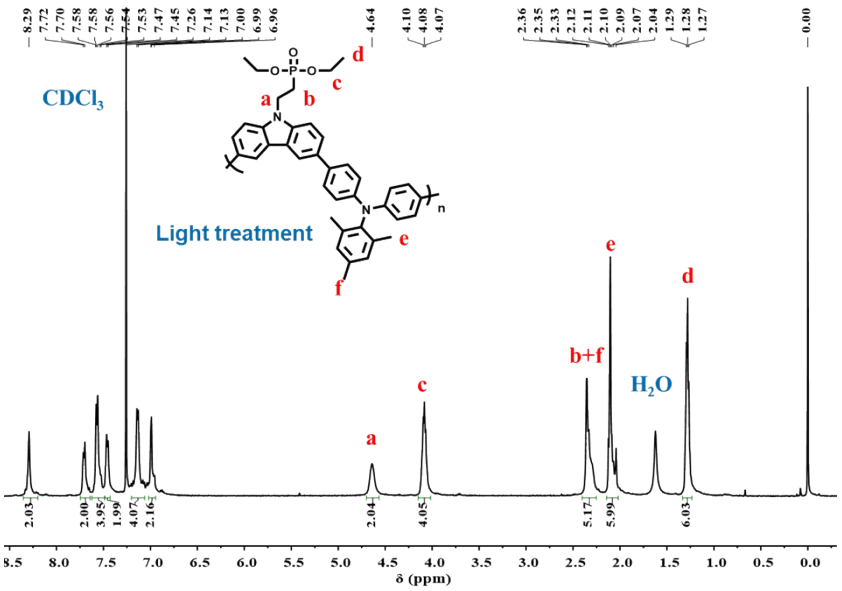

Figure S12. ^{1}H NMR spectrum of the PTACz-PO after light treatment for 10 min.

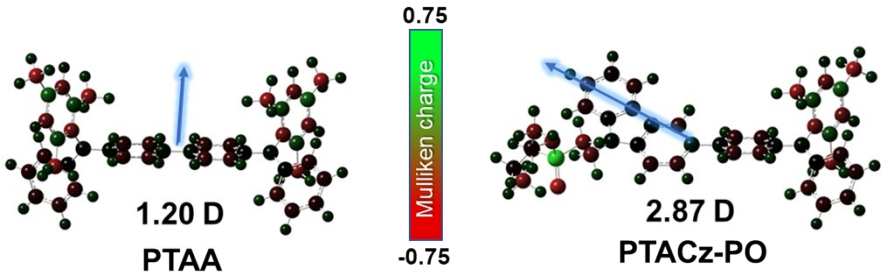

Figure S13. Dipole moments of the molecular models, simulating repeat unit, for the PTAA and PTACz-PO, with blue arrows indicating the directions.

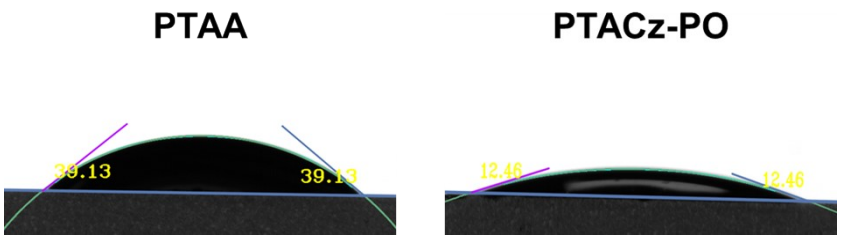

Figure S14. The contact angle images of PTAA and PTACz-PO with perovskite solution.

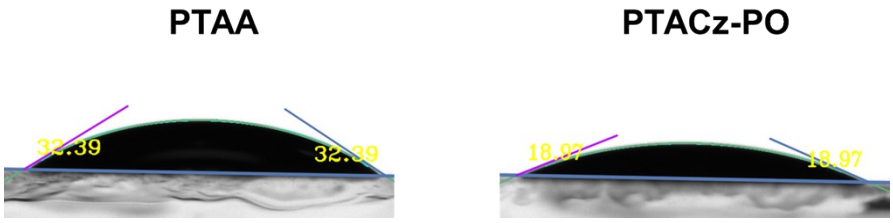

Figure S15. The contact angle images of PTAA and PTACz-PO with diiodomethane atop.

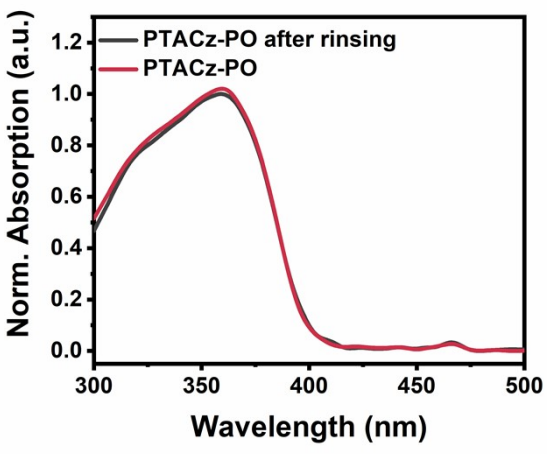

Figure S16. Normalized UV–vis absorption spectra of PTACz-PO film and PTACz-PO after rinsing with mixed solvent (DMF:DMSO = 4:1).

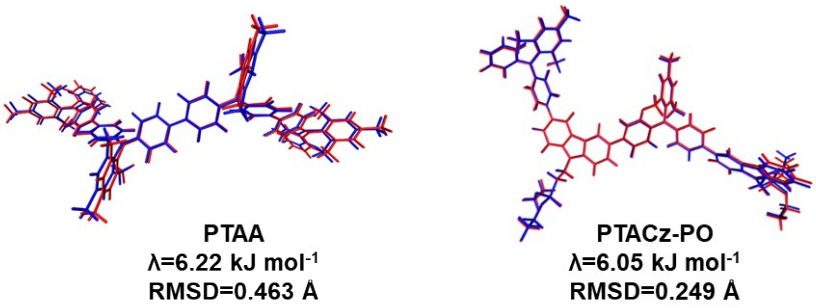

Figure S17. Comparison of structural relaxation between the ground state (blue) and excited state (red) for PTAA and PTACz-PO dimers, with RMSD values and reorganization energy λ indicated.

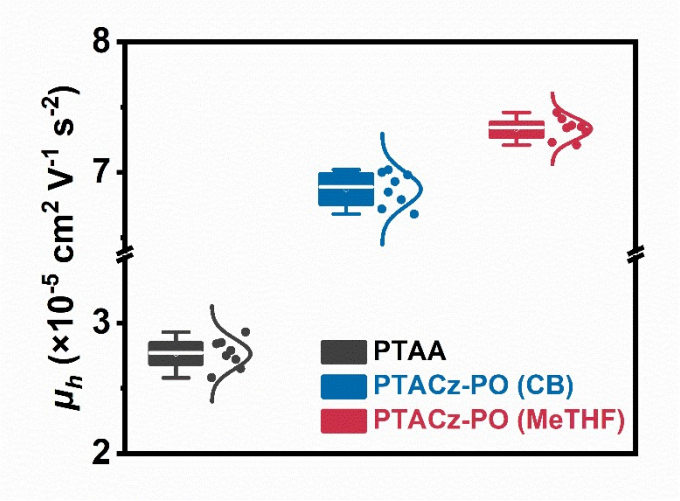

Figure S18. The distribution of hole mobility values for polymer HTMs, measured by SCLC methods.

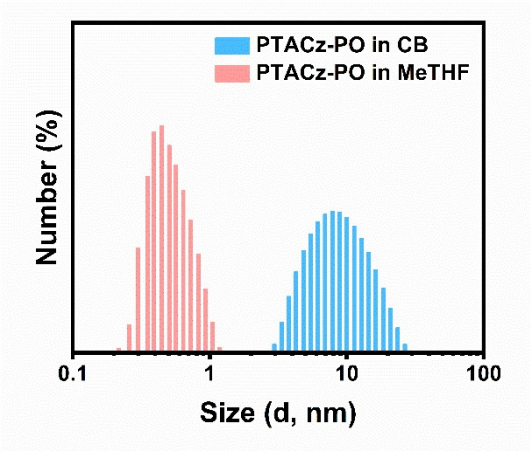

Figure S19. Size distribution of PTACz-PO in different solvent.

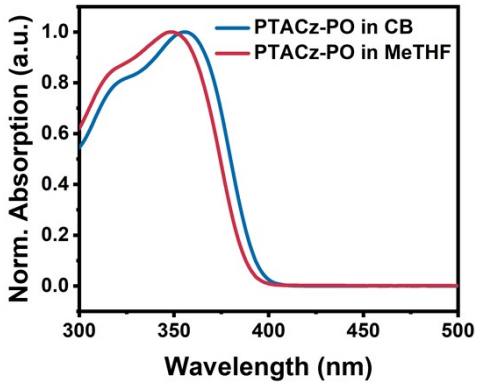

Figure S20. Normalized UV–vis absorption spectra of PTACz-PO in different solvents.

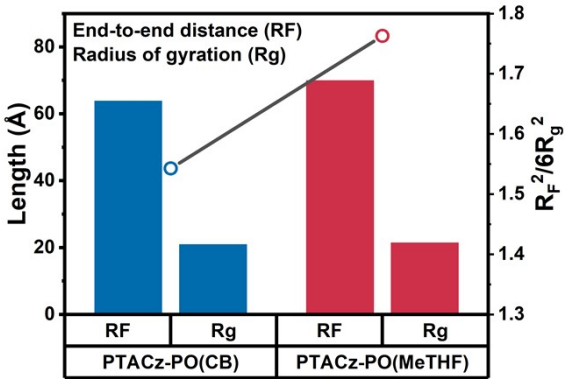

Figure S21. End-to-end distance (R_F), radius of gyration (R_g) and $R_F^2/6R_g^2$ for the polymer chains.

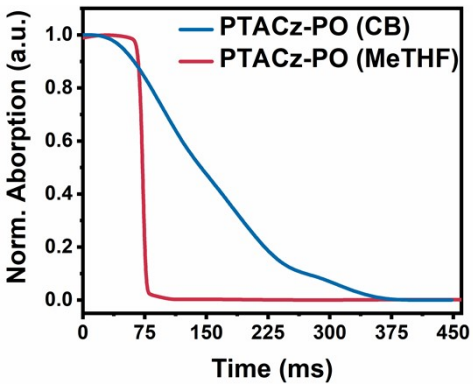

Figure S22. Normalized absorption of peaks for CB processing PTACz-PO and MeTHF processing PTACz-PO from 0 to 470 ms.

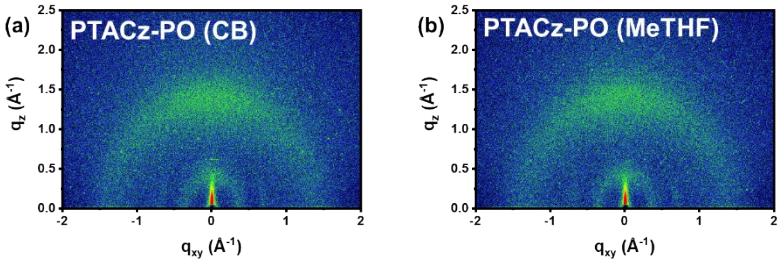

Figure S23. GIWAXS images of a) CB-processed PTACz-PO and b) MeTHF-processed PTACz-PO thin films.

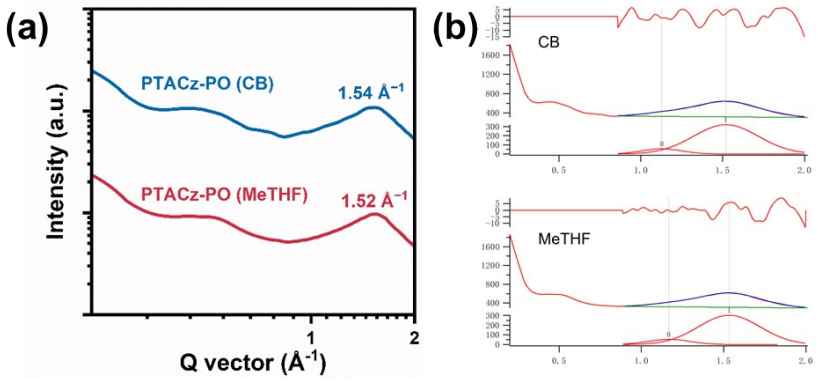

Figure S24. (a) The corresponding 1D intensity profiles along the out of plane direction. (b) Multi-peak fitting of the π–π stacking reflections in the OOP direction of PTACz-PO thin films prepared from CB and MeTHF. All the peaks were fitted with Gaussian functions.

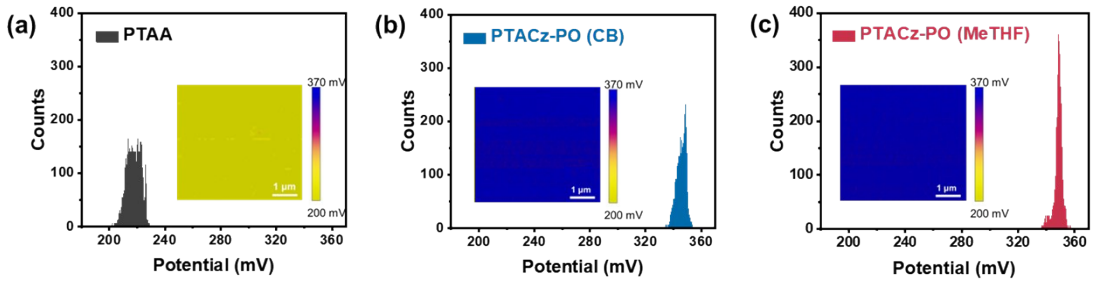

Figure S25. Surface potential difference distribution of HTMs measured through KPFM. Insert: KPFM image of ITO/polymer HTMs.

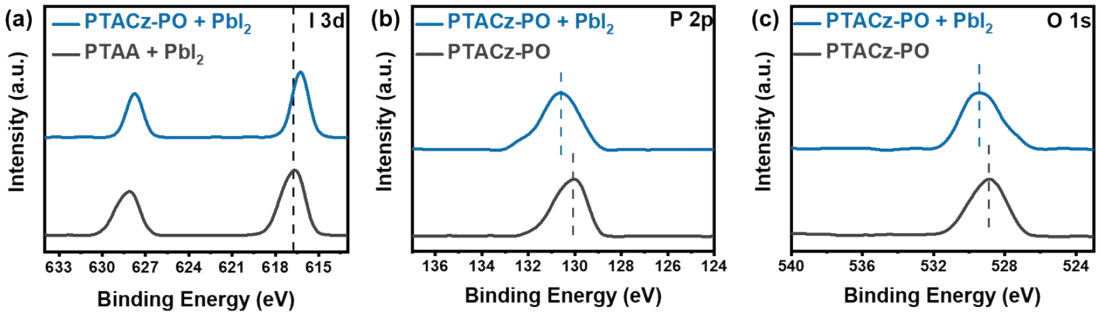

Figure S26. (a) I 3d, (b) P 2p and (c) O 1s XPS spectra of polymer HTMs+PbI_2 films and polymer HTMs films.

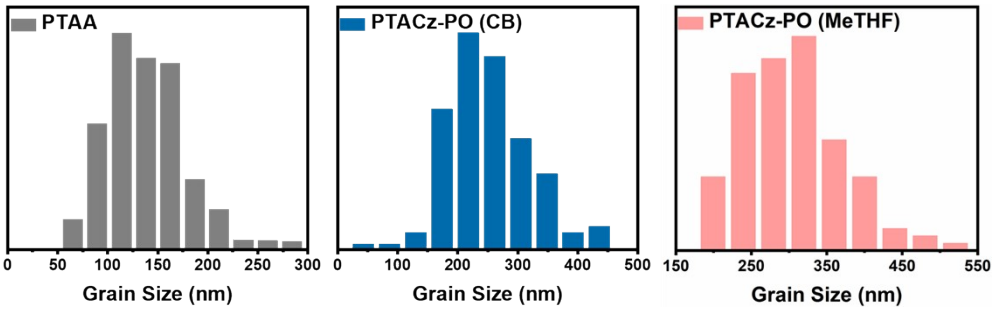

Figure S27. Grain size distribution of perovskites spin-coated on PTAA, CB-processed PTACz-PO and MeTHF-processed PTACz-PO, respectively. This distribution was extracted from the SEM images for the top of perovskites.

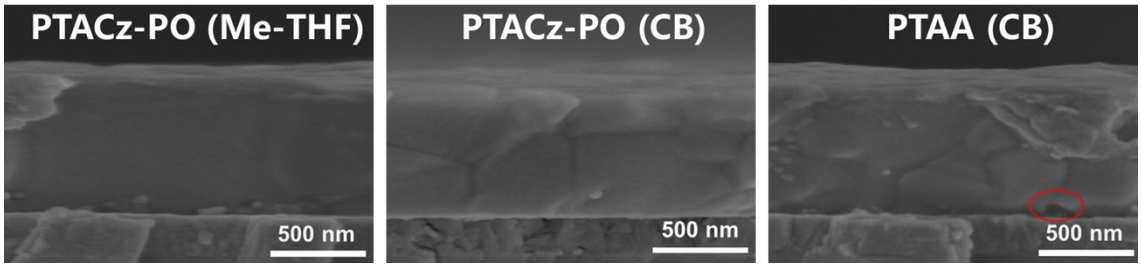

Figure S28. FESEM cross-sectional images (b) of perovskite films on different HTMs.

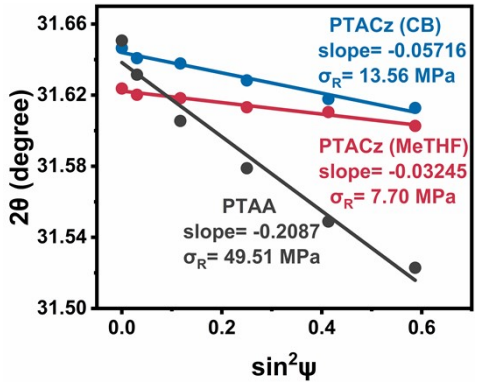

Figure S29. The residual strain of the corresponding diffraction peaks (2θ) of perovskite films on studied HTL as a function of $\sin^2\psi$.

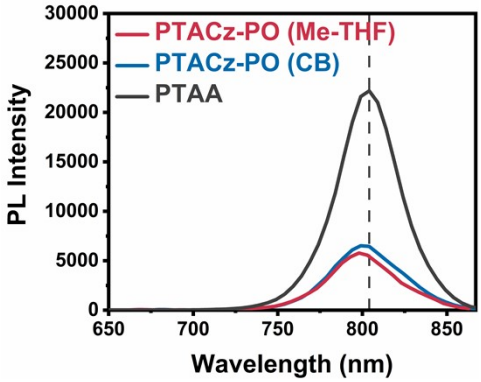

Figure S30. Steady PL spectra of ITO/HTMs /Perovskite.

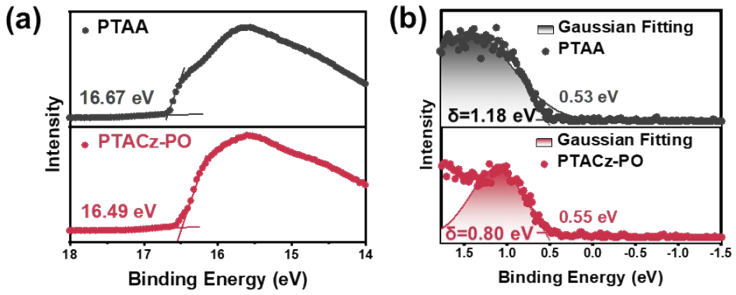

Figure S31. UPS spectra showing the cutoff regions (a) and Fermi edge (b).

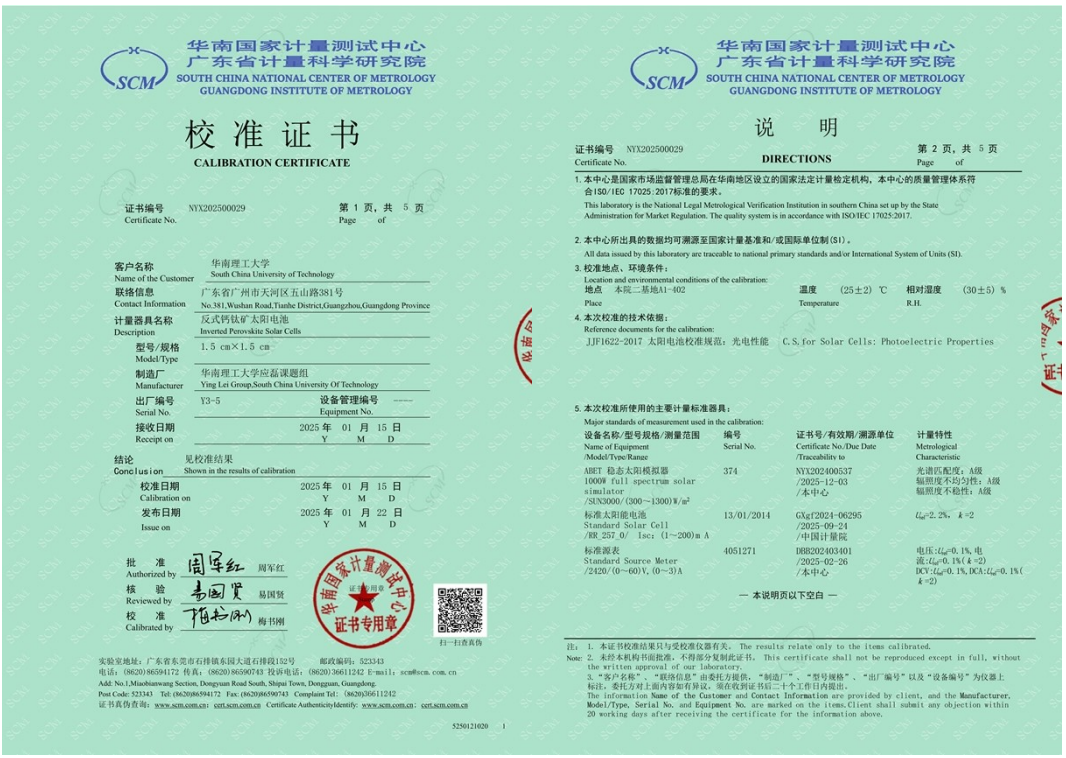

华南国家计量测试中心
广东省计量科学研究院
SOUTH CHINA NATIONAL CENTER OF METROLOGY
GUANGDONG INSTITUTE OF METROLOGY

校 准 证 书
CALIBRATION CERTIFICATE

证书编号 Certificate No. NYX202500029 第 1 页，共 5 页 Page of

客户名称 Name of the Customer 华南理工大学 South China University of Technology
联络信息 Contact Information 广东省广州市天河区五山路381号 No.381,Wushan Road,Tianhe District,Guangzhou,Guangdong Province
计量器具名称 Description 反式钙钛矿太阳电池 Inverted Perovskite Solar Cells
型号/规格 Model/Type 1.5 cm×1.5 cm
制造厂 Manufacturer 华南理工大学应磊课题组 Ying Lei Group,South China University Of Technology
出厂编号 Serial No. Y3-5 设备管理编号 Equipment No. ----
接收日期 Receipt on 2025 年 01 月 15 日 Y M D
结论 Conclusion 见校准结果 Shown in the results of calibration
校准日期 Calibration on 2025 年 01 月 15 日 Y M D
发布日期 Issue on 2025 年 01 月 22 日 Y M D

批 准 Authorized by 周军红
核 验 Reviewed by 易国贤
校 准 Calibrated by 梅书刚

华南国家计量测试中心 证书专用章

扫一扫查真伪

实验室地址：广东省东莞市石排镇东园大道石排段182号 邮政编码：523343
电话：(8620)86594172 传真：(8620)86590743 投诉电话：(8620)36611242 E-mail：scm@scm.com.cn
Add: No.1,Miaobiaowang Section, Dongyuan Road South, Shipai Town, Dongguan, Guangdong.
Post Code: 523343 Tel: (86)(20)86594172 Fax: (86)(20)86590743 Complaint Tel: (86)(20)36611242
证书真伪查询：www.scm.com.cn；cert.scm.com.cn Certificate Authenticity Identify: www.scm.com.cn；cert.scm.com.cn

5250121020 1

华南国家计量测试中心
广东省计量科学研究院
SOUTH CHINA NATIONAL CENTER OF METROLOGY
GUANGDONG INSTITUTE OF METROLOGY

说 明
DIRECTIONS

证书编号 Certificate No. NYX202500029 第 2 页，共 5 页 Page of

1. 本中心是国家市场监督管理总局在华南地区设立的国家法定计量检定机构，本中心的质量管理体系符合ISO/IEC 17025:2017标准的要求。
This laboratory is the National Legal Metrological Verification Institution in southern China set up by the State Administration for Market Regulation. The quality system is in accordance with ISO/IEC 17025:2017.

2. 本中心所出具的数据均可溯源至国家计量基准和/或国际单位制(SI)。
All data issued by this laboratory are traceable to national primary standards and/or International System of Units (SI).

3. 校准地点、环境条件：
Location and environmental conditions of the calibration:
地点 Place 本院二黑地1-402 温度 Temperature (25±2) ℃ 相对湿度 R.H. (30±5) %

4. 本次校准的技术依据：
Reference documents for the calibration:
JJF1622-2017 太阳电池校准规范；光电性能 C.S. for Solar Cells: Photoelectric Properties

5. 本次校准所使用的主要计量标准器具：
Major standards of measurement used in the calibration:

设备名称/型号规格/测量范围 Name of Equipment /Model/Type Range	编号 Serial No.	证书号/有效期/溯源单位 Certificate No./Due Date /Traceability to	计量特性 Metrological Characteristic
ABET 稳态太阳模拟器 1000# full spectrum solar simulator /SUN3000/(300～1300)W/m²	374	NYX202400537 /2025-12-03 /本中心	光谱匹配度：A级 辐照度不均匀性：A级 辐照度不稳性：A级
标准太阳能电池 Standard Solar Cell /RR_257_0/ Isc：(1～200)m A	13/01/2014	GXgf2024-06295 /2025-09-24 /中国计量院	U_{rel}=2.2%，k=2
标准源表 Standard Source Meter /2420/(0～60)V,(0～3)A	4051271	DBB202403401 /2025-02-26 /本中心	电压:U_{rel}=0.1%,电流:U_{rel}=0.1%(k=2) DCV:U_{rel}=0.1%,DCA:U_{rel}=0.1%(k=2)

— 本说明页以下空白 —

注： 1. 本证书校准结果只与受校准仪器有关。 The results relate only to the items calibrated.
Note: 2. 未经本机构书面批准，不得部分复制此证书。 This certificate shall not be reproduced except in full, without the written approval of our laboratory.
3. "客户名称"、"联络信息"由委托方提供，"制造厂"、"型号规格"、"出厂编号"以及"设备编号"为仪器上标注。委托方对上面内容如有异议，须在收到证书后二十个工作日内提出。
The information Name of the Customer and Contact Information are provided by client, and the Manufacturer, Model/Type, Serial No. and Equipment No. are marked on the items.Client shall submit any objection within 20 working days after receiving the certificate for the information above.

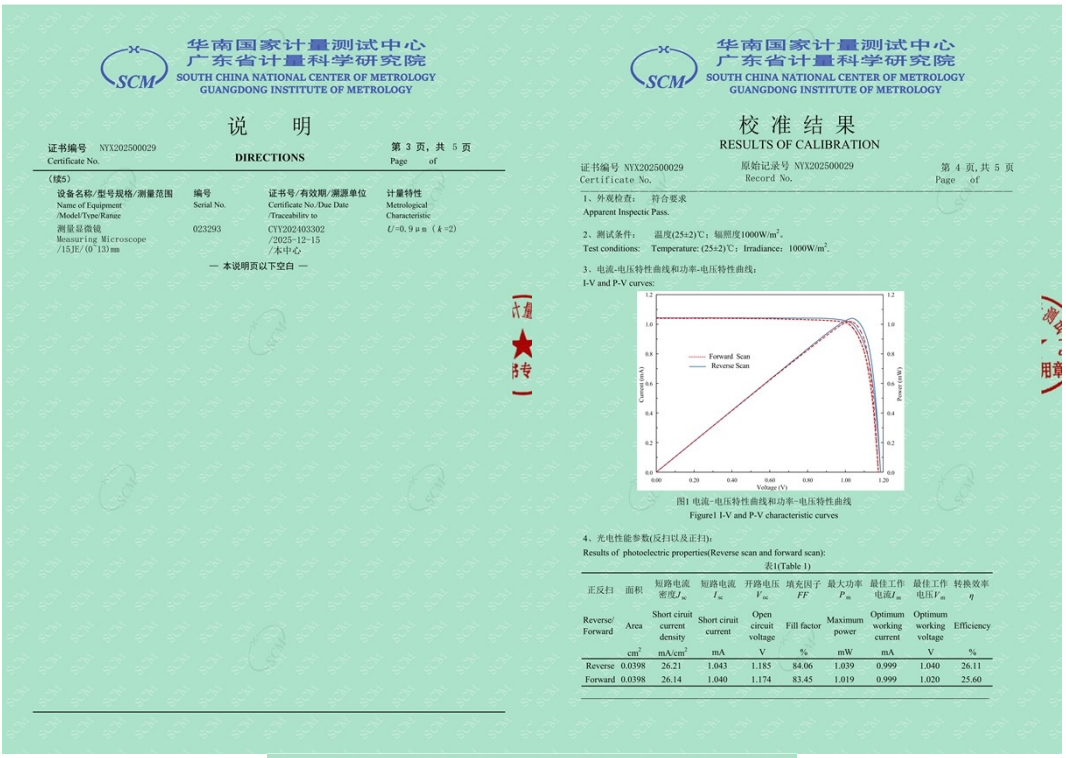

华南国家计量测试中心
广东省计量科学研究院
SOUTH CHINA NATIONAL CENTER OF METROLOGY
GUANGDONG INSTITUTE OF METROLOGY

说　明

证书编号 NYX202500029
Certificate No.

DIRECTIONS

第 3 页，共 5 页
Page of

（续5）

设备名称/型号规格/测量范围 Name of Equipment /Model/Type/Ranne	编号 Serial No.	证书号/有效期/溯源单位 Cerificate No./Due Date /Traceability to	计量特性 Metrological Characteristic
测量显微镜 Measuring Microscope /15JE/(0~13)mm	023293	CIY202403302 /2025-12-15 /本中心	U=0.9 μm（k=2）

— 本说明页以下空白 —

华南国家计量测试中心
广东省计量科学研究院
SOUTH CHINA NATIONAL CENTER OF METROLOGY
GUANGDONG INSTITUTE OF METROLOGY

校 准 结 果
RESULTS OF CALIBRATION

证书编号 NYX202500029
Certificate No.

原始记录号 NYX202500029
Record No.

第 4 页，共 5 页
Page of

1、外观检查： 符合要求
Apparent Inspectic Pass.

2、测试条件： 温度(25±2)℃；辐照度1000W/m^2。
Test conditions: Temperature: (25±2)℃; Irradiance: 1000W/m^2.

3、电流-电压特性曲线和功率-电压特性曲线：
I-V and P-V curves:

图1 电流-电压特性曲线和功率-电压特性曲线
Figure1 I-V and P-V characteristic curves

4、光电性能参数(反扫以及正扫)：
Results of photoelectric properties(Reverse scan and forward scan):

表1(Table 1)

正反扫 Reverse/ Forward	面积 Area	短路电流密度J_{sc} Short ciruit current density	短路电流 I_{sc} Short circuit current	开路电压 V_{oc} Open circuit voltage	填充因子 FF Fill factor	最大功率 P_m Maximum power	最佳工作电流I_m Optimum working current	最佳工作电压V_m Optimum working voltage	转换效率 η Efficiency
	cm^2	mA/cm^2	mA	V	%	mW	mA	V	%
Reverse	0.0398	26.21	1.043	1.185	84.06	1.039	0.999	1.040	26.11
Forward	0.0398	26.14	1.040	1.174	83.45	1.019	0.999	1.020	25.60

华南国家计量测试中心
广东省计量科学研究院
SOUTH CHINA NATIONAL CENTER OF METROLOGY
GUANGDONG INSTITUTE OF METROLOGY

校 准 结 果
RESULTS OF CALIBRATION

证书编号 NYX202500029
Certificate No.

原始记录号 NYX202500029
Record No.

第 5 页，共 5 页
Page of

5、被测样品信息：
Sample information:

图2 测试中使用的掩膜板及被测样品正面照片
Figure 2 Mask used during measurement and obverse side of the sample

图3 被测样品反面照片
Figure 3 Reverse side of the sample

金属掩膜板光阑平均尺寸： 1.994 mm × 1.995 mm
The average size of metal aperture mask:

说明(Note)：
1、被测样品的有效辐照面积基于对金属掩模板光阑的测量。
The effective illuminated area of the measured sample based on the measurement of metal aperture mask.
2、本次测量结果的扩展不确定度为：开路电压V_{oc}：U_{rel}=1.2%，短路电流I_{sc}：U_{rel}=2.7%，最大功率P_{max}：U_{rel}=3.0%，转换效率η：U_{rel}=3.4%，(k=2)。
The expanded uncertainty of measuring results: V_{oc}: U_{rel}=1.2%, I_{sc}: U_{rel}=2.7%, P_{max}: U_{rel}=3.0%, η:U_{rel}=3.4%，(k=2)。
3、校准活动中对测量结果有影响的条件：温度:(25±2)℃，湿度:(30±5)%RH。
Conditions under which the calibrations were made that have an influence on the measurement results: Temperature:(25±2)℃, Humidity:(30±5)%RH.
4、本证书中给出的扩展不确定度依据JJF1059.1-2012《测量不确定度评定与表示》评定，由合成标准不确定度乘以包含概率约为95%时对应的包含因子k得到。
The expanded uncertainty given in this certificate is evaluated according to JJF 1059.1-2012"*Evaluation and Expression of Uncertainty in Measurement*",which is obtained by multiplying the combined standard uncertainty by the coverage factor k corresponding to the coverage probability of about 95%.
5、该仪器的溯源日期为本证书的"校准日期"，由于复校时间间隔的长短是由仪器的使用情况、使用者、仪器本身质量等诸因素所决定的，因此，送校单位可根据实际使用情况自主决定复校时间间隔。更换重要部件、维修或对仪器性能有怀疑时，应及时校准。
The traceability date of this instrument is the "Calibration Date"on this certificate, Since the calibration interval is determined by the use of the instrument,oneration of the user, the quality of the instrument itself and other factors，the re-calibration date can decided by the user according to the actual situation.In case of replacement of important parts,maintenance or doubt on the performance of the instrument,it shall be calibrated in time.

Figure S32. Efficiency certification report for champion devices of IPSC.

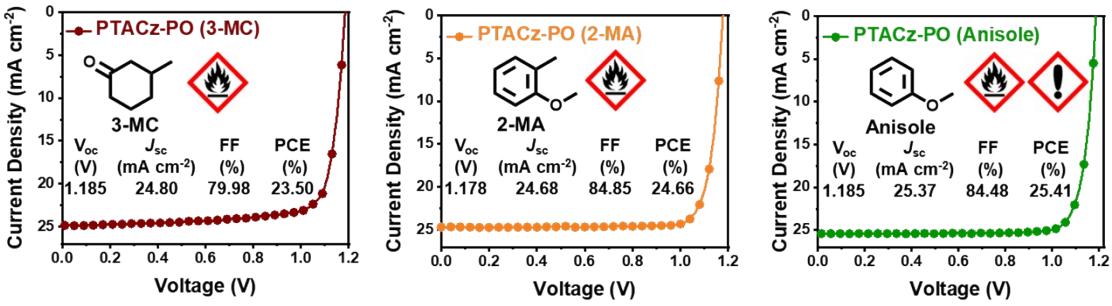

Figure S33. *J–V* curves of perovskite solar cells using other green solvents processing PTACz-PO as HTL (insert: photovoltaic performance of perovskite solar cells).

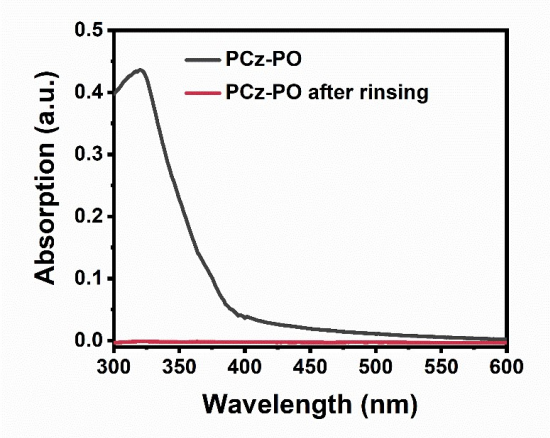

Figure S34. Normalized UV–vis absorption spectra of PCz-PO film and PCz-PO after rinsing with the mixed solvent (DMF:DMSO = 4:1).

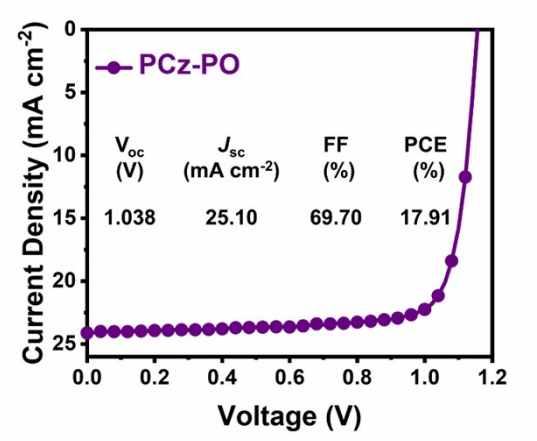

Figure S35. *J–V* curves of 0.04 cm^2 perovskite solar cells using PCz-PO as HTL (insert: photovoltaic performance of perovskite solar cells).

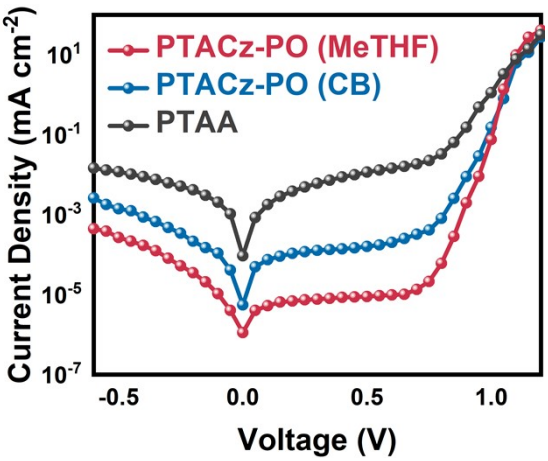

Figure S36. Dark current test for the device based on different HTMs.

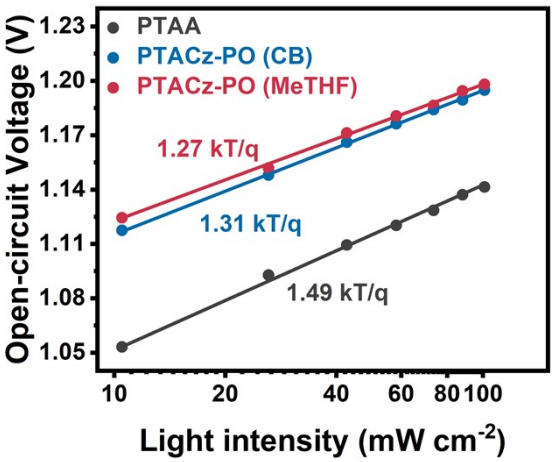

Figure S37. Light-intensity dependent V_{OC} of perovskite solar cells using PTAA, CB-processed PTACz-PO, and MeTHF-processed PTACz-PO as HTMs, respectively.

Table S1. The molecular weight of the polymer HTMs measured by GPC.

HTMs	M_n (kDa)	M_w (kDa)	Đ
PTAA	6.0	7.5	1.3
PTACz-PO	9.4	13.7	1.5

Table S2. Solubility test of PTAA and PTACz-PO with various solvents.

	Solvent	PTAA	PTACz-PO	Photographs of PTAA (left) and PTACz-PO (right)

1	Ethyl acetate	0	3	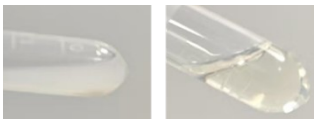
2	Chloroform	3	3	
3	Chlorobenzene	3	3	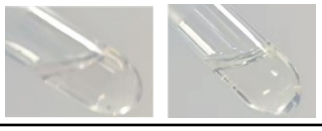
4	Toluene	3	3	
5	Ethanol	0	0	
6	Methanol	0	0	
7	p-Xylene	3	3	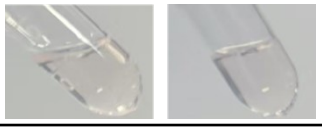
8	Cyclohexane	0	0	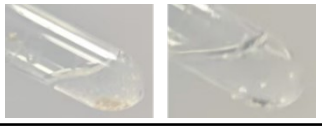
9	1,4-dioxane	0	3	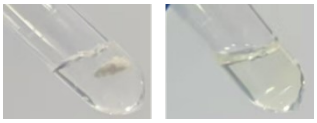
10	Isopropyl alcohol	0	0	
11	Acetonitrile	0	0	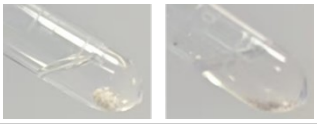
12	Acetone	0	3	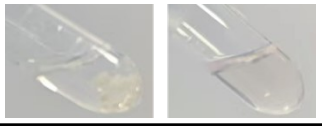
13	Anisole	3	3	
14	Cyclopentyl methyl ether	0	3	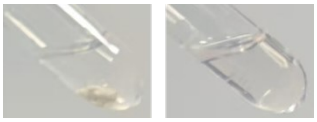

15	2-Methyltetrahydrofuran	0	3	
16	2-ethyl-hexanol	0	3	

0-insoluble; 3- soluble.

Table S3. Solubility distances (R_a) and relative energy differences (RED = R_a/R_0) of PTAA in MeTHF and PTACz-PO in different solvents.

HTMs (Solvent)	R_a	RED
PTAA (MeTHF)	5.36	1.05
PTACz-PO (MeTHF)	1.69	0.26
PTACz-PO (CB)	5.66	0.87
PTACz-PO (DMF)	10.89	1.61
PTACz-PO (DMSO)	17.64	2.71

Table S4. Fitting results of TRPL characteristics for perovskites fabricated on different polymer HTMs.

HTMs	τ_1 (ns)	A_1 (%)	τ_2 (ns)	A_2 (%)	τ_{ave} (ns)
PTAA	93.37	96.48	470.90	3.52	152.03
PTACz-PO (CB)	126.30	81.85	669.80	18.15	420.01
PTACz-PO (MeTHF)	176.62	81.09	1110.79	18.91	732.01

Table S5. Series resistance (R_s) and recombination resistance (R_{sh}) of the fitting for

different polymer HTMs-based perovskite solar cell.

HTMs	R_s	R_{sh}
PTAA	145.8	15.6
PTACz-PO (CB)	51.9	31.7
PTACz-PO (MeTHF)	20.6	37.1

Table S6. Summary of PCE and FF of inverted PSCs with PCE>20% based on polymer HTM reported in the literatures.

HTMs	Perovskite composition	V_{OC} (V)	PCE (%)	Ref.	Year
p-PY	$Cs_{0.05}(FA_{0.9}MA_{0.1})_{0.95}Pb(I_{0.9}Br_{0.1})_3$	1.153	22.40	3	2022
TFB	$MAPbI_3$	1.090	20.20	4	2018
PPE2	$(FAPbI_3)_{0.83}(MAPbBr_3)_{0.17}$	1.180	21.31	5	2020
PFDTS	$Cs_{0.15}FA_{0.85}PbI_3$	1.082	20.15	6	2021
BNs-F	$MAPbI_3$	1.083	20.56	7	2022
p-PFICZ	$Cs_{0.15}FA_{0.85}PbI_3$	1.091	21.39	8	2023
PTAA-P1	$Cs_{0.05}(FA_{0.98}MA_{0.02})_{0.95}Pb(I_{0.98}Br_{0.02})_3$	1.170	24.89	9	2023
DEG-PTAA	$(FAPbI_3)_{0.95}(CsPbBr_3)_{0.05}$	1.120	22.26	10	2023
PFDT-2F-COOH	$FA_{0.93}MA_{0.07}PbI_3$	1.111	21.68	11	2020
Poly-4PACz	$Cs_{0.05}(FA_{0.98}MA_{0.02})_{0.95}Pb(I_{0.98}Br_{0.02})_3$	1.170	24.40	12	2023
PBTI-BTP	$(FA_{0.17}MA_{0.94}PbI_{3.11})_{0.95}(PbCl_2)_{0.05}$	1.162	22.02	13	2024
PTTI-TPA	$(FA_{0.17}MA_{0.94}PbI_{3.11})_{0.95}(PbCl_2)_{0.05}$	1.100	21.00	14	2021

PsTA-mPV	$FA_{0.83}Cs_{0.17}Pb_{2.7}Br_{0.3}$	1.094	20.21	15	2022
BN-12	$MAPbI_3$	1.078	20.28	16	2022
2MeO-PTAA	$MAPbI_3$	1.080	20.23	17	2022
PTAAO6	$Cs_{0.05}(FA_{0.95}MA_{0.05})_{0.95}Pb(I_{0.95}Br_{0.05})_3$	1.192	25.19	18	2024
Poly-DBPP	$MA_{0.7}FA_{0.3}PbI_3$	1.18	25.1	19	2024
Poly-DCPA	$MA_{0.7}FA_{0.3}PbI_3$	1.17	24.9	20	2024
PF8ICz	$Cs_{0.05}(FA_{0.95}MA_{0.05})_{0.95}Pb(I_{0.95}Br_{0.05})_3$	1.19	25.4	21	2024
CP4	$Cs_{0.05}(FA_{0.98}MA_{0.02})_{0.95}Pb(I_{0.98}Br_{0.02})_3$	1.2	26.21	22	2024
PTACz-PO	$Cs_{0.05}(FA_{0.95}MA_{0.05})_{0.95}Pb(I_{0.95}Br_{0.05})_3$	1.211	26.31	**This work**	

References

1 R. Chen, S. Liu, X. Xu, F. Ren, J. Zhou, X. Tian, Z. Yang, X. Guanz, Z. Liu, S. Zhang, Y. Zhang, Y. Wu, L. Han, Y. Qi and W. Chen, *Energy Environ. Sci.*, **2022**, 15, 2567–2580.

2 Z. Ren, S. Luo, X. Shi, Y. Dou, T. Liu, L. Wang, K. Tsang, F. Wang, Y. Zhao, Y. Liu, X. Hu, X. Peng, W. Liu, H. Yan and S. Chen, *Sci. China Chem*., **2024**, 67, 1941–1945.

3 X. J. Xu, X. Y. Ji, R. Chen, F. Y. Ye, S. J. Liu, S. Zhang, W. Chen, Y. Z. Wu and W. H. Zhu, *Adv. Funct. Mater.*, **2022**, 32, 2109968.

4 D. Yang, T. Sano, Y. Yaguchi, H. Sun, H. Sasabe and J. Kido, *Adv. Funct. Mater.*, **2019**, 29, 1807556.

5 X. Sun, X. Deng, Z. Li, B. Xiong, C. Zhong, Z. Zhu, Z. Li and A. K. Jen, *Adv. Sci.*, **2020**, 7, 1903331.

6 C. Chen, Z. N. Song, C. X. Xiao, D. W. Zhao, N. Shrestha, C. W. Li, G. Yang, F. Yao, X. L. Zheng, R. J. Ellingson, C. S. Jiang, M. A. Jassim, K. Zhu, G. J. Fang and

Y. F. Yan, *J. Mater. Chem. A.*, **2022**, 10, 3159-3168.

7 M. Luo, X. P. Zong, M. Zhao, Z. Sun, Y. Chen, M. Liang, Y. Z. Wu and S. Xue, *Chem. Eng. J.*, **2022**, 442, 136136.

8 L. Wan, Y. Zhao, Y. L. Tan, L. Y. Lou, Z. S. Wang, *Chem. Eng. J.*, 2023, 455, 140569.

9 X. Wu, D. Gao, X. Sun, S. Zhang, Q. Wang, B. Li, Z. Li, M. Qin, X. Jiang, C. Zhang, Z. Li, X. Lu, N. Li, S. Xiao, X. Zhong, S. Yang, Z. Li and Z. Zhu, *Adv. Mater.*, **2023**, 35, 2208431.

10 C. Lim, Y. Kim, S. Lee, H. H. Park, N. J. Jeon and B. J. Kim, *J. Mater. Chem. A.*, **2023**, 11, 6615-6624.

11 L. Wan, W. Zhang, S, Fu, L. Chen, Y. Wang, Z. Xue, Y. Tao, W. Zhang, W. Song and J. Fang, *J. Mater. Chem. A.*, **2020**, 8, 6517-6523.

12 Z. Ren, Z. Cui, X. Shi, L. Wang, Y. Dou, F. Wang, H. Lin, H. Yan and S. Chen, *Joule.*, **2023**, 7, 2894-2904.

13 B. Li, J. Yang, Q. Liao, X. Ji, Y. Wang, J. Yang, B. Liu, Q. Liang, Z. Wang, H. Li, K. Wang, H. Sun, L. Niu and X. Guo, *Sol. RRL.*, **2024**, 8, 2300740.

14 B. Li, K. Yang, Q. Liao, Y. Wang, M. Su, Y. Li, Y. Shi, X. Feng, J. Huang, H. Sun and X. Guo, *Adv. Funct. Mater.*, **2021**, 31, 2100332.

15 M. Li, J. Chang, R. Sun, H. Wang, Q. Tian, S. Chen, J. Wang, Q. He, G. Zhao, W. Xu, Z. Li, S. Zhang, F. Wang and T. Qin, *ACS Appl. Mater. Interfaces.*, **2022**, 14, 53331-53339.

16 M. Luo, X. Zong, W. Zhang, M. Hua, Z. Sun, M. Liang and S. Xue, *ACS Appl. Mater. Interfaces.*, **2022**, 14, 31285-31295.

17 C. Wang, Q. Xiong, Z. Zhang, L. Meng, F. Li, L. Yang, X. Wang, Q. Zhou, W. Fan, L. Liang, S. Lien, X. Li, J. Wu and P. Gao, *ACS Appl. Mater. Interfaces.*, **2022**, 14, 12640–12651.

18 S. Yin, X. Luo, F. Tang, W. Zhong, W. Yang, Z. Xiong, Y. Lin, F. Peng and L. Ying, *Adv. Energy Mater.*, **2024**, 2404575.

19 F. Wang, T. Liu, Y. Liu, Y. Zhou, X. Dong, Y. Zhang, X. Shi, Y. Dou, Z. Ren, L.

Wang, Y. Zhao, S. Luo, X. Hu, X. Peng, C. Bao, W. Wang, J. Wang, W. Hu, S. Chen, *Adv. Mater.*, **2024**, 36, 2412059.

20 Y. Zhao, Y. Liu, Z. Ren, Y. Li, Y. Zhang, F. Kong, T. Liu, X. Shi, Y. Dou, L. Wang, F. Wang, X. Guo, Y. Cao, W. Wang, P. C. Y. Chow, S. Chen, *Energy Environ. Sci.*, **2025**, 18, 1366-1374.

21 X. Luo, S. Yin, Z. Xiong, G. Qian, Y. Lin, N. Li, L. Ying, *Small*, **2025**, 21, 2409284.

22 L. Zhan, S. Zhang, Z. Li, W. Li, H. Zhang, J. He, X. Ji, S. Liu, F. Yu, S. Wang, Z. Ning, Z. Li, M. Stolterfoht, L. Han, W.-H. Zhu, Y. Xu, Y. Wu, *Angew. Chem. Int. Ed.*, **2025**, e202422571.